Deep levels generated by thermal oxidation in p-type 4H-SiC

AUTHOR(S):

Kawahara, Koutarou; Suda, Jun; Kimoto, Tsunenobu

CITATION:

Kawahara, Koutarou ...[et al]. Deep levels generated by thermal oxidation in p-type 4H-SiC. Journal of Applied Physics 2013, 113(3): 033705.

ISSUE DATE:

2013-01-17

URL:

http://hdl.handle.net/2433/187956

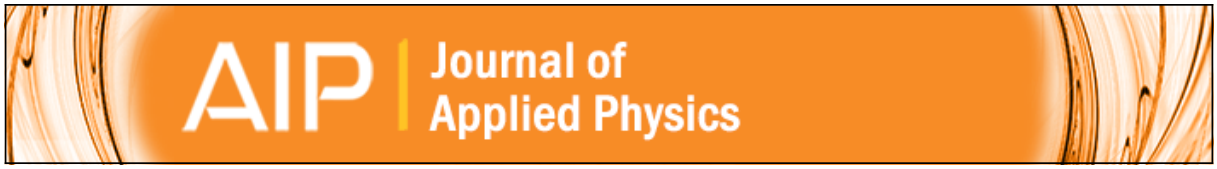

Deep levels generated by thermal oxidation in p-type 4H-SiC

Koutarou Kawahara, Jun Suda, and Tsunenobu Kimoto

Citation: Journal of Applied Physics **113**, 033705 (2013); doi: 10.1063/1.4776240
View online: http://dx.doi.org/10.1063/1.4776240
View Table of Contents: http://scitation.aip.org/content/aip/journal/jap/113/3?ver=pdfcov
Published by the AIP Publishing

JOURNAL OF APPLIED PHYSICS **113**, 033705 (2013)

Deep levels generated by thermal oxidation in p-type 4H-SiC

Koutarou Kawahara,[a] Jun Suda, and Tsunenobu Kimoto[b]
Department of Electronic Science and Engineering, Kyoto University, Katsura, Nishikyo, Kyoto 615-8510, Japan

(Received 15 November 2012; accepted 28 December 2012; published online 17 January 2013)

Thermal oxidation is an effective method to reduce deep levels, especially the $Z_{1/2}$-center ($E_C - 0.67$ eV), which strongly suppresses carrier lifetimes in n-type 4H-SiC epilayers. The oxidation, however, simultaneously generates other deep levels, HK0 ($E_V + 0.79$ eV) and HK2 ($E_V + 0.98$ eV) centers, within the lower half of the bandgap of SiC, where the HK0 center is a dominant deep level with a concentration of about 1×10^{13} cm^{-3} after oxidation. By comparing deep levels observed in three sets of p-type 4H-SiC: oxidized, electron-irradiated, and C^+- or Si^+-implanted samples, we find that the HK0 and HK2 centers are complexes including carbon interstitials such as the di-carbon interstitial or di-carbon antisite. Other defects observed in p-type 4H-SiC after electron irradiation or after C^+/Si^+ implantation are also studied. © *2013 American Institute of Physics*.
[http://dx.doi.org/10.1063/1.4776240]

I. INTRODUCTION

In producing high-power, high-temperature, and high-frequency devices, SiC is one of the most fascinating semiconductors. Deep levels in the SiC epilayers, however, prevent the development of high-performance SiC bipolar devices. The deep levels work as recombination centers resulting in the reduction of carrier lifetimes[1] and also work as carrier traps, leading to the reduction in conductivity. Therefore, deep levels, especially the $Z_{1/2}$ center,[2] a "lifetime killer" in n-type 4H-SiC,[3,4] must be controlled.

In recent years, two effective methods were found to reduce the $Z_{1/2}$ center: (i) C^+ implantation followed by Ar annealing[5,6] and (ii) thermal oxidation.[7] In both, excess carbon atoms induced by C^+ implantation/oxidation diffuse into the deeper region of a SiC epilayer during post-implantation annealing/oxidation and fill carbon vacancies (V_C).[6–8] The $Z_{1/2}$ center most likely contains V_C,[9–12] and based on photo-EPR and electrical characterization[13,14] the origin has recently been identified as the acceptor levels of V_C. The $Z_{1/2}$ concentration is thus strongly reduced by these processes (C^+ implantation and thermal oxidation), leading to very long carrier lifetimes ($20 - 30\mu$s) in n-type SiC.[15,16]

In contrast, new deep levels, HK0 ($E_V + 0.79$ eV) and HK2 ($E_V + 0.98$ eV) centers, are observed after thermal oxidation or C^+ implantation, which are probably related to the interstitials diffusing from the SiO_2/SiC interface (oxidation) or from the implanted region (C^+ implantation).[7,8] Although effects of HK0 and HK2 centers on carrier lifetimes are negligible compared with the $Z_{1/2}$ center,[8] these can affect lifetimes when the $Z_{1/2}$ centers are eliminated. In addition, investigation of the generated defects, the HK0 and HK2 centers, should lead us to a comprehensive understanding of the $Z_{1/2}$ reduction mechanism by thermal oxidation or C^+ implantation, which is required for full control of carrier lifetimes in SiC epilayers.

In this study, we compare depth profiles and thermal stability of the HK0 and HK2 centers in three sets of p-type 4H-SiC: (i) oxidized, (ii) electron-irradiated, and (iii) C^+- or Si^+-implanted samples, and discuss the origins of these traps.

II. EXPERIMENTS

The starting materials were Al-doped p-type 4H-SiC (0001) epilayers (12 μm thickness with acceptor concentration (N_a) of 7×10^{15} cm^{-3}, or 120 μm thickness with N_a of 7×10^{14} cm^{-3}). (i) The first set of samples was oxidized at different temperatures (1150, 1200, 1300, and 1400 °C) for various periods (1.3–16.5 h) in 100% oxygen ambient, whereas (ii) the second set of samples was irradiated with 150 keV electrons (fluence: 1.0×10^{17} cm^{-2}). (iii) The third set of samples was implanted with 10–50 keV carbon (or 25–110 keV silicon) ions with a total dose of 1×10^{13} cm^{-2} or 1×10^{14} cm^{-2} (implanted atom concentration: 1×10^{18} cm^{-3} or 1×10^{19} cm^{-3}), forming a 140-nm-box-profile. The C^+-implanted (or Si^+-implanted) samples were annealed in Ar ambient at various temperatures (1000, 1300, 1440, 1500, 1700, and 1800 °C) for 20 min. For deep level transient spectroscopy (DLTS) measurements, Ti was employed as Schottky contacts (typical diameter: 1 mm). The backside ohmic contacts were made of a Ti/Al/Ni (20 nm/100 nm/80 nm) layer annealed at 1000 °C for 2 min. A period width of 0.205 s was employed in all DLTS measurements performed in this study. The depth profiles of trap concentrations up to 10 μm were measured by changing the reverse bias voltage up to 100 V in the DLTS measurements. To monitor deeper regions (over 10 μm), the samples were mechanically polished from the surfaces, and the DLTS measurements were repeated. Additional deep levels, though, did not appear by polishing.

[a]Electronic mail: kawahara@semicon.kuee.kyoto-u.ac.jp.
[b]Also at Photonics and Electronics Science and Engineering Center (PESEC), Kyoto University, Katsura, Nishikyo, Kyoto 615-8510, Japan.

III. RESULTS AND DISCUSSION

A. Deep levels after thermal oxidation

Figure 1 shows the DLTS spectra obtained from a depth of ~4 μm for an as-grown sample before and after thermal oxidation at 1300 °C for 15.9 h. In the as-grown sample, GP1 ($E_V + 0.46$ eV) and D ($E_V + 0.63$ eV) centers were observed. The GP1 center is located at a deeper level than the boron acceptor (shallow boron level, $E_V + (0.26 - 0.39)$ eV (Refs. 17 and 18)). In contrast, the D center is a well-known deep level in p-type 4H-SiC ($E_V + (0.54 - 0.73)$ eV),[17–20] which has been attributed to a boron atom in a silicon site with an adjacent carbon vacancy (B_{Si}-V_C).[18,21,22] After oxidation, the D center disappeared, whereas the HK0 ($E_V + 0.79$ eV) and HK2 ($E_V + 0.98$ eV) centers appeared. The HK0 and HK2 centers are both observed in RIE-etched samples[20,23] and electron-irradiated samples[20] after Ar annealing (950–1000 °C), whereas the HK2 center is detected occasionally in as-grown samples.[20] Because these two centers are observed after thermal oxidation, the two deep levels may be related to the C (or Si) interstitials diffusing from the SiO_2/SiC interface during the oxidation.

1. Comparison between experimental defect profiles and calculated interstitial profiles after thermal oxidation

Figure 2 shows depth profiles of the HK0 center after oxidation at various temperatures for 1.3 h. When oxidation is conducted at higher temperatures, the defect concentration is higher and the HK0 center is distributed to a deeper region, which is consistent with an expected distribution of interstitials after diffusion from the SiO_2/SiC interface. In Ref. 8, we introduced a calculation model for C_I diffusion and recombination with V_C during thermal oxidation, and showed that depth profiles of the $Z_{1/2}$ center after oxidation can be predicted using the model. In this study, however, it is very difficult to propose an accurate diffusion model for calculation of the HK0 distributions because (i) V_C concentration (and the distribution) in p-type SiC is not known, and (ii) as discussed in the Sec. III A 2 the HK0 center may originate from a C-interstitial complex rather than a single interstitial. Thus, for the calculation of the HK0 distributions, we

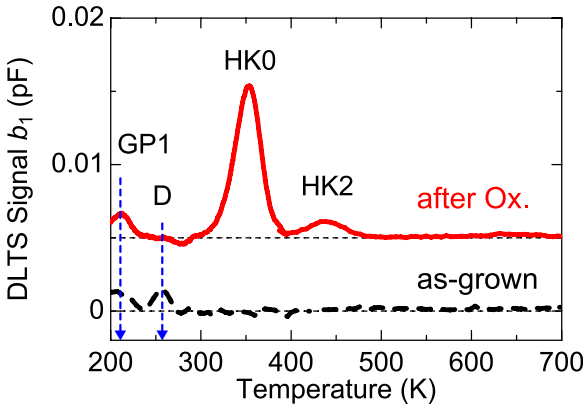

FIG. 1. DLTS spectra for the as-grown p-type 4H-SiC (dashed line) before and after thermal oxidation at 1300 °C for 15.9 h (solid line).

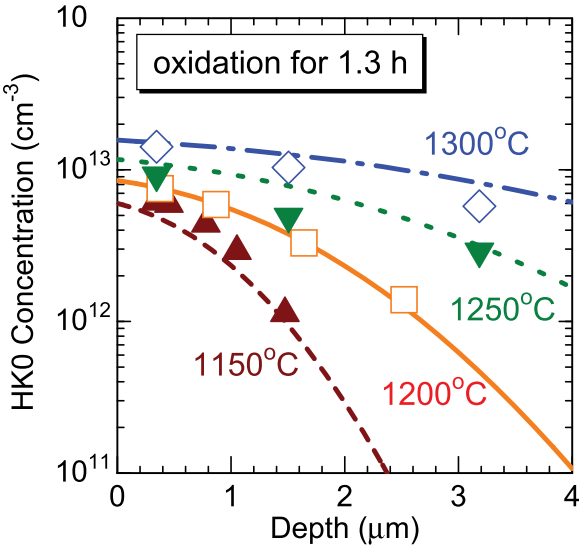

FIG. 2. Depth profiles of HK0 center after oxidation at various temperatures for 1.3 h. Each symbol indicates the experimental data and each line indicates the calculated n_I distribution obtained from Eqs. (1)–(5).

use a simple model that defects (interstitials) diffuse from the SiO_2/SiC interface into the SiC bulk during oxidation.

Denoting the concentration of interstitials (C_I or Si_I) by n_I and the diffusion coefficient of the interstitials by D, the distribution of interstitials after oxidation is found by solving the diffusion equations

$$\frac{\partial n_I}{\partial t} = D \cdot \frac{\partial^2 n_I}{\partial x^2}, \tag{1}$$

where the boundary and initial conditions are fixed as

$$-D \cdot \frac{\partial n_I}{\partial x}\Big|_{x=0} = F_0 \cdot t^{-\alpha} (t \neq 0), \tag{2}$$

$$n_I|_{t=0} = 0. \tag{3}$$

When the calculated results are compared with the experiments, fitting parameters, $D_\infty, E_{aD}, F_{0\infty}$, and E_{aF}, are obtained from

$$D = D_\infty \cdot \exp\left(-\frac{E_{aD}}{kT}\right), \tag{4}$$

$$F_0 = F_{0\infty} \cdot \exp\left(-\frac{E_{aF}}{kT}\right). \tag{5}$$

The boundary condition, Eq. (2) determines the interstitial emission at the oxidation interface, which is described with F_0. Because the oxidation rate slows with time, the gradual decrease in flux of the emitted interstitials as oxidation (time) proceeds was taken into account by introducing a damping coefficient α. This constant ($\alpha = 1$ at "$t_{ox} < 0.8$h," $\alpha = 0.23$ at "$0.8\text{h} < t_{ox}$") was determined from the dependence of the oxidation rate on oxidation time at different oxidation temperatures (not shown, details given elsewhere[8]). From Eqs. (4) and (5), D and F_0 are described as functions of temperature. The fitting parameters, E_{aD} and E_{aF}, signify the respective activation energies corresponding to the energy

barriers for the migration and the generation of interstitials. The lines in Fig. 2 indicate the calculated n_I distribution obtained from Eqs. (1)–(5). Fitting parameters determined in this study for the HK0 distributions are listed in Table I. Note that the parameters in Table I can be referred only as a guide because of the simplification of the calculation model.

With these parameters, the dependence of the HK0 distribution on oxidation time can also be fitted. Figure 3 shows the depth profiles of the HK0 center after oxidation at 1300 °C for 1.3–15.9 h. Longer oxidation leads to a deeper HK0 distribution. Here, 5.3 h × 3 in Fig. 3 (squares and dotted line) indicates that the oxides were removed by hydrofluoric acid treatment after every 5.3 h of oxidation, which enhances the oxidation speed compared with continuous oxidation because, as mentioned above, the oxidation rate slows with time. Using the same parameters listed in Table I, the calculated results can reproduce the enhancement in HK0 generation by repeated oxidation and oxide removal. At depths shallower than 1 μm, the calculation results for the 15.9 h and 5.3 h × 3 oxidation show slightly lower HK0 concentration than the experimental results. It is, however, very difficult to propose a modified diffusion model to explain the defect concentration near the surface because of the reason mentioned above. Because the calculation (lines) almost fit the experimental data (symbols), the inference is that the origin of the HK0 center must contain interstitials diffusing from the SiO_2 interface during oxidation. The origin of the diffusing atoms (Si or/and C) is discussed in the next sections.

2. Specific behaviors of the HK0 center during oxidation and subsequent Ar annealing

We found that neither generation nor diffusion of the HK0 center itself occurs by Ar annealing at temperature lower than 1300 °C. Figure 4 shows depth profiles of the HK0 center after oxidation at 1150 °C for 1.3 h, and after oxidation followed by Ar annealing at 1150 °C for 4.3 h. The HK0 distribution did not change by the subsequent annealing at 1150 °C in an Ar atmosphere, which indicates that the HK0 center does not diffuse by Ar annealing at 1150 °C. That HK0 diffuses during oxidation and not during Ar annealing can be explained as a diffusion of interstitials during oxidation generated at the SiO_2/SiC interface and forming more stable defects, which become the source for the HK0 center, and thereby terminating the diffusion. Therefore, rather than a single interstitial, the origin of the HK0 center could be a complex such as an interstitial cluster or an interstitial-impurity complex. From *ab initio* calculations, the formation of a carbon di-interstitial ($(C_I)_2$) seems to be energetically favorable for a pair of carbon interstitials,[24–27]

TABLE I. Parameter values obtained by fitting of the interstitial profiles calculated based on the diffusion equations (Eqs. (1)–(5)) to experimental HK0 profiles shown in Fig. 1. The top row indicates the "X" in the first column.

	D	F_0
Activation energy E_{aX}	3.6 eV	2.9 eV
Coefficient X_∞	1.4 $cm^2 s^{-1}$	1.4 × 10^{18} $cm^{-2} s^{\alpha-1}$

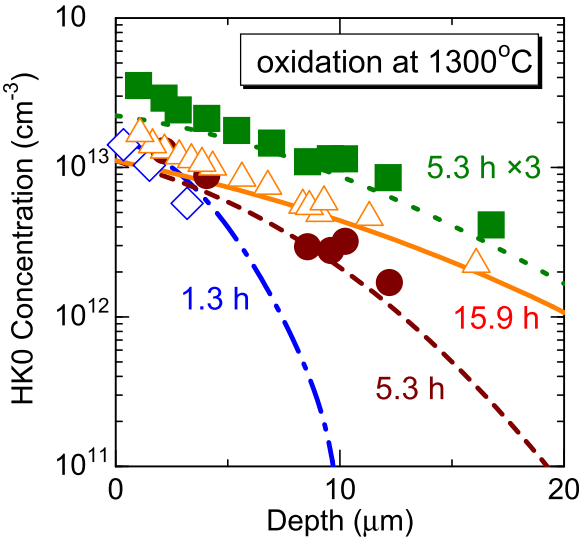

FIG. 3. Depth profiles of the HK0 center after oxidation at 1300 °C for 1.3–15.9 h. Each symbol indicates the experimental data and each line indicates the calculated n_I distribution obtained from Eqs. (1)–(5).

and that the $(C_I)_2$ defect forms energy levels at 0.1–1.2 eV above the valence band edge in the lower half of the bandgap of 4 H-SiC,[24,26,28] which does not conflict with the energy level of the HK0 ($E_V + 0.79$ eV) center detected by DLTS. The energy levels of the carbon di-interstitial ($(C_I)_2$) obtained by *ab initio* calculation[24,26,28] are shown in Fig. 5, which indicates that the $(C_I)_2$ is a candidate as source for the HK0 center.

The HK0 center is not stable at temperatures higher than 1400 °C. Figure 6 shows the DLTS spectra of the sample after thermal oxidation at 1300 °C for 15.9 h, and after the oxidation followed by Ar annealing at 1500 °C for 2 h. All deep levels including the HK0 center disappeared after the subsequent Ar annealing at 1500 °C (the HK0 center disappears at temperatures over 1400 °C (Refs. 20, 29, and 30)). The dotted line in Fig. 6 shows the DLTS spectrum of the

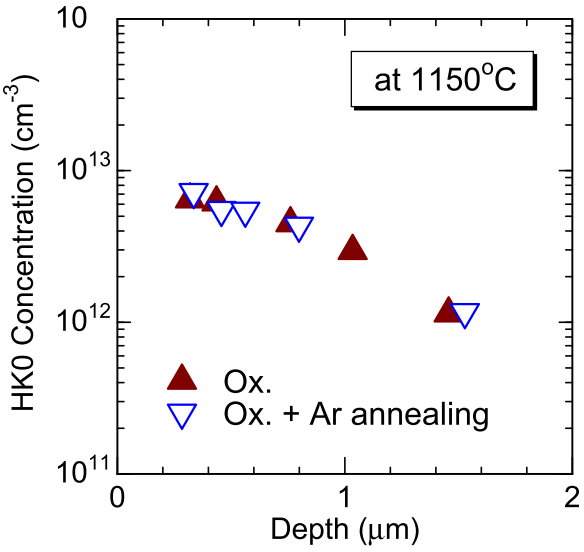

FIG. 4. Depth profiles of the HK0 center after oxidation at 1150 °C for 1.3 h (closed triangles), and after the oxidation followed by Ar annealing at 1150 °C for 4.3 h (reverse triangles).

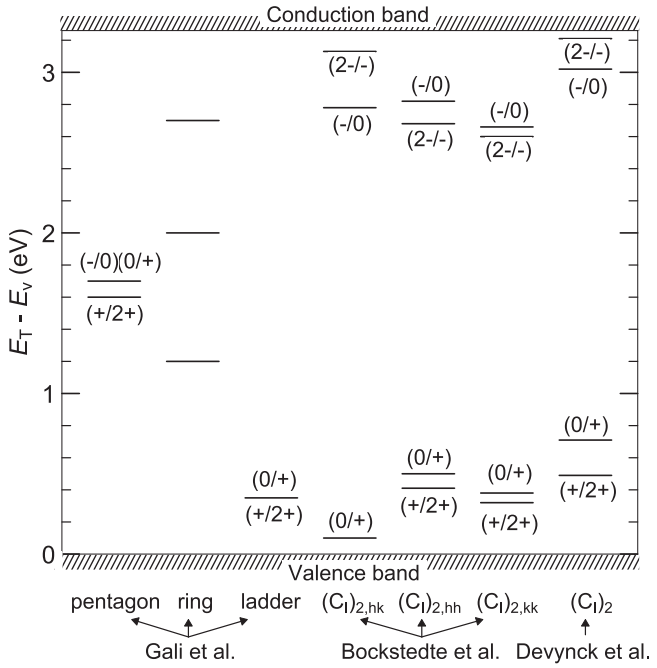

FIG. 5. Energy levels of carbon di-interstitial ($(C_I)_2$) obtained by *ab initio* calculation.[24,26,28]

sample after thermal oxidation at 1400 °C for 16.5 h. In contrast with the oxidation at 1300 °C, the HK0 and HK2 centers were not generated by the high-temperature oxidation at 1400 °C. If the origin of the HK0 center is assumed to be an interstitial complex, as previously mentioned, these results (in Fig. 6) indicate that at temperatures over 1400 °C excess interstitial atoms exist as (i) single interstitials (the origin of HK0 center is dissociated and diffuses at the high temperature), or (ii) more thermally stable defects possessing higher binding energy than that of origin of the HK0 center.

In the last decade, interstitial complexes in SiC have extensively been investigated by photoluminescence (PL),[31–36] and these results have been compared with *ab initio* calculations.[25,32,35,37] Several kinds of C-related defects have been suggested to exist in electron-irradiated 4H-SiC and 6H-SiC.[31–37] The identified PL signals are: T1 (a center), T2/T3 (b center), and T4 (c center) centers as $(C_2)_{Si}$,[33–36] U center (471.8 nm zero phonon line (ZPL) in 4H-SiC) as $(C_3)_{Si}$,[32,33,36] G center (493.5 nm ZPL in 4 H-SiC) as $((C_2)_{Si})_2$,[33,36] Z center (maybe 599.3 nm ZPL in 4 H-SiC) as $(C_I)_2$.[32,33] The dissociation energy was calculated to be about 5.5 eV for $(C_I)_2$,[24–26] 3.6 eV for $(C_2)_{Si}$,[25] 5.8 eV for $(C_3)_{Si}$,[25] and 6.7 eV for $((C_2)_{Si})_2$,[25] which is consistent with relatively high thermal stability of the defect centers observed in PL.[33] Note that post-irradiation annealing behaviors of the U center (ZPL at 471.8 nm in 4 H-SiC) and the G center (ZPL at 493.5 nm in 4H-SiC) are similar with that of the HK0 center detected by DLTS in this study. The U/G centers appear after annealing at 1100 °C/950 °C, remain at 1300 °C/1200 °C, and disappear at 1400 °C/1300 °C (all annealing is 30 min long),[33] whereas the HK0 center appears after annealing at 950 °C, remains at 1300 °C, and disappears at 1400 °C.

Therefore, the origin of the HK0 center could be $(C_I)_2$, $(C_3)_{Si}$, or $((C_2)_{Si})_2$, which is formed from single carbon interstitials generated and diffusing during oxidation at lower than 1300 °C. $(C_3)_{Si}$ and $((C_2)_{Si})_2$ can be formed when the diffusing carbon atoms occupy silicon vacancies or displace silicon atoms.

B. Deep levels generated by electron irradiation

As described in the last section, the origin of the HK0 center could be carbon-related complexes. To obtain more insights of the origin, we investigated p-type samples irradiated with 150 keV electrons (fluence: 1.0×10^{17} cm^{-2}), where displacement of only the carbon atoms occurs.[9,12] Figure 7 shows DLTS spectra of the samples after electron irradiation and after subsequent oxidation at 1150 °C for 1.3 h. UK1 ($E_V + 0.49$ eV),[20] HS2 ($E_V + 0.63$ eV),[9,20] UK2 ($E_V + 0.71$ eV),[20] and HK4 ($E_V + 1.4$ eV)[20] centers were detected after electron irradiation. The HS2 center has been reported to appear after electron irradiation with the energy of 116 keV–9 MeV,[9,20] whereas the UK1 and UK2 centers appear with 160 keV–400 keV electrons.[20] The HK4 center has also been observed in as-grown samples.[20] As evident in Fig. 7, after subsequent oxidation at 1150 °C for 1.3 h, the HS2 and HK4 centers disappear, and the HK0 and HK2 centers emerge. The HK0 and HK2 centers cannot originate

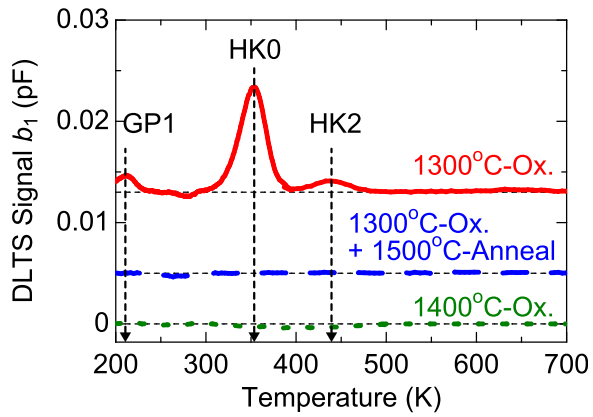

FIG. 6. DLTS spectra of the p-type 4 H-SiC after thermal oxidation at 1300 °C for 15.9 h (solid line), and after the oxidation followed by Ar annealing at 1500 °C for 2 h (dashed line). DLTS spectrum of the sample after thermal oxidation at 1400 °C for 16.5 h is also shown as a dotted line.

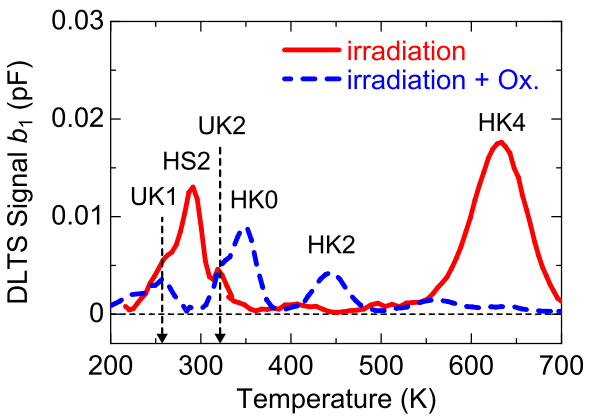

FIG. 7. DLTS spectra of the p-type 4 H-SiC irradiated with 150 keV electrons (solid line), and after electron irradiation followed by oxidation at 1150 °C for 1.3 h (dashed line).

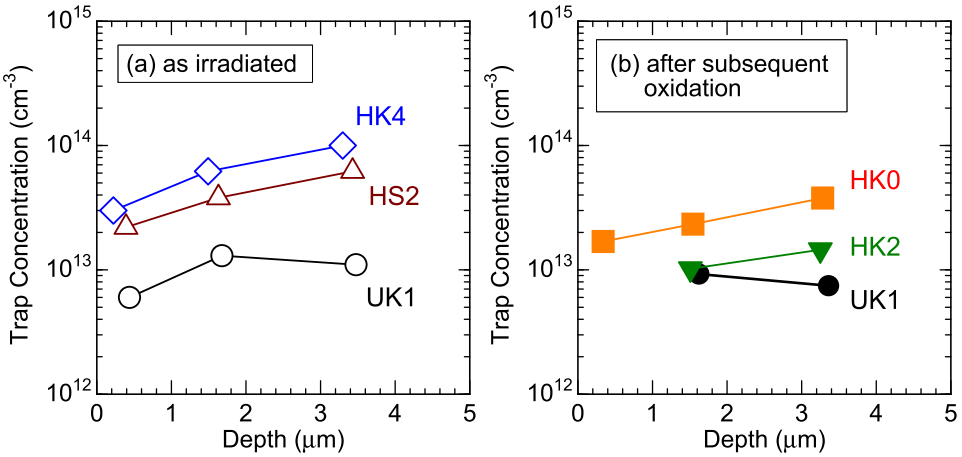

FIG. 8. Depth profiles of (a) UK1 (circles), HS2 (triangles), and HK4 (rhombuses) centers in the p-type 4 H-SiC after electron irradiation (150 keV, 1.0×10^{17} cm^{-2}), and (b) HK0 (squares) and HK2 (reverse triangles) centers after irradiation followed by thermal oxidation at 1150 °C for 1.3 h.

from a single interstitial because the HK0 and HK2 centers were not detected in as-irradiated samples but in samples after subsequent oxidation (or Ar annealing[20]).

Figure 8 shows depth profiles of (a) UK1, HS2, and HK4 centers in the p-type 4 H-SiC after electron irradiation, and (b) HK0 and HK2 centers after the irradiation followed by thermal oxidation at 1150 °C for 1.3 h. The HK0 center after electron irradiation followed by thermal oxidation shows higher concentration and is distributed to a deeper region compared with the HK0 center after only thermal oxidation (Fig. 2), which means that irradiation-induced damage is the main cause of the HK0 generation in these samples. Figure 9 shows depth profiles of the HK0 center in the samples after electron irradiation followed by thermal oxidation at different temperatures for 1.3 h. The HK0 distribution in the samples after electron irradiation followed by thermal oxidation is almost independent of oxidation temperature, which also means that the HK0 center generated by thermal oxidation is negligible compared with the HK0 generation caused by irradiation damage.

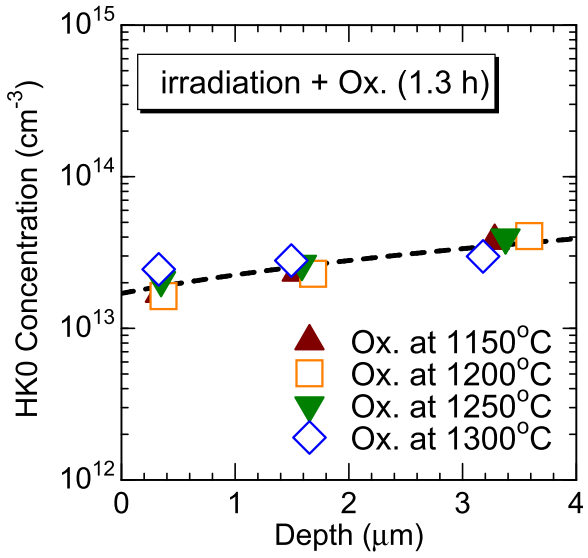

FIG. 9. Depth profiles of the HK0 center in the p-type 4H-SiC after electron irradiation (150 keV, 1.0×10^{17} cm^{-2}) followed by thermal oxidation at different temperatures for 1.3 h.

The other four deep levels, UK1, HS2, HK2, and HK4, show similar distribution to the HK0 distribution (Fig. 8), which may indicate that these also originate from irradiation-induced damage (related to C_I or/and V_C). The HK0 and HK2 centers were detected only after post-irradiation annealing, whereas the UK1, HS2, and HK4 centers were detected just after electron irradiation. Therefore, the origin of the HK0 center (and the HK2 center) should be a carbon-related complex defect (and not single interstitial), which is consistent with the results obtained in the last section.

C. Deep levels generated by C^+ or Si^+ implantation

Investigation on the deep levels in C^+- or Si^+-implanted samples must be helpful for clarifying the origin of the deep levels. Therefore, C^+ or Si^+ implantation was performed on the p-type SiC epilayers, followed by Ar annealing. Figure 10 shows DLTS spectra of the p-type 4 H-SiC after C^+ implantation followed by Ar annealing at 1300 °C (the solid line is the signal obtained near the surface (<1 μm), and the dashed line in a deeper region) and at 1500 °C (dotted line). In the C^+-implanted samples, the same deep levels, UK1, UK2, HK0, and HK2 centers, are observed as those observed in the electron-irradiated samples (Fig. 7) that must be related to the carbon displacement as discussed above. When the

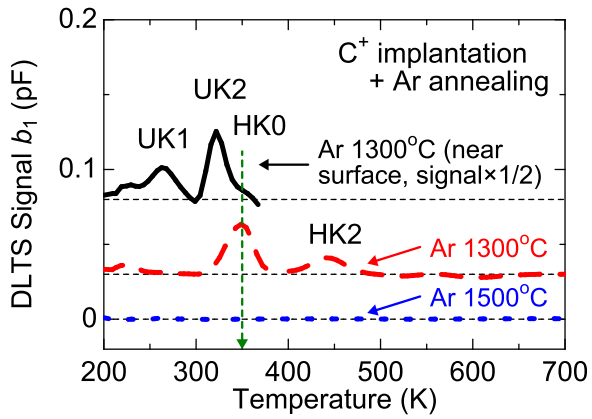

FIG. 10. DLTS spectra of the p-type 4 H-SiC after C+ implantation followed by Ar annealing at 1300 °C (solid line is the signal obtained near the surface (<1 μm), and dashed line in the deeper region) and 1500 °C (dotted line).

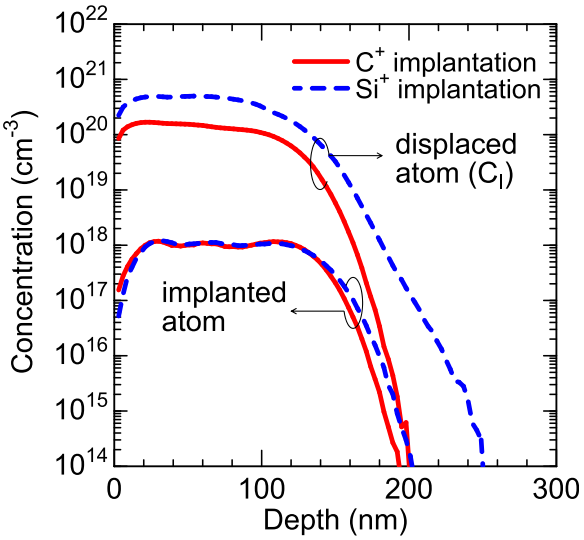

FIG. 11. Depth profiles of implanted atoms and carbon interstitials after C^+ or Si^+ implantation (total dose: 1×10^{13} cm^{-2}) simulated by SRIM code.

temperature of the subsequent annealing was 1500 °C, no DLTS peaks could be observed as indicated in Fig. 10 by the dotted line. This is consistent with the results obtained in the oxidized samples where all DLTS peaks disappeared after annealing over 1400 °C (Fig. 6). For Si^+ implantation, a similar behavior for the deep levels was observed (not shown).

Figure 11 shows the depth profiles of implanted atoms and C_I generated by the collision of implanted ions, just after implantation, which were simulated using a SRIM code;[38] SRIM is an acronym for stopping and range of ions in matter. The C_I concentration in the Si^+-implanted samples is higher than that in the C^+-implanted samples due to the higher energy of Si^+ implantation (10–50 keV for C^+ implantation and 25–110 keV for Si^+ implantation) and larger mass of Si^+. The distribution of V_C/V_{S_i} is almost the same as that of C_I/Si_I in the simulation (the difference is within 1 nm, not shown), which means that carbon atoms/silicon atoms are not knocked far away from their original positions by collisions with implanted atoms. In contrast, the distribution of Si_I and V_{S_i} shows a little lower concentration (~70%) than that of C_I (and V_C) because of the higher displacement energy of 35 eV for a silicon atom compared with 21 eV for a carbon atom.[39] Note that a large amount of the interstitials and vacancies generated by implantation bombardment should recombine during the subsequent Ar annealing because these are located closely to each other after implantation.

Figure 12 shows the depth profiles of deep levels in the (a) C^+- or (b) Si^+-implanted samples followed by Ar annealing at 1300 °C for 20 min, respectively. Depth profiles of carbon interstitials just after C^+ or Si^+ implantation simulated by the SRIM code are also shown as a solid line in the same figures. The deep levels can be categorized into two groups; the UK1 and UK2 centers as group A, and the HK0 and HK2 centers as group B. Group A has low diffusivity, the distribution of which is not much different from that of C_I (or the other intrinsic defects just after ion implantation) simulated by the SRIM code (the real tail region of the C_I distribution should spread to a deeper region because the SRIM code assumes a completely amorphous material as a target). Therefore, the UK1 and UK2 centers could originate from immobile defect(s) induced by collision of implanted atoms (e.g., vacancy and complex). The similarity in the depth profiles of the UK1 and UK2 centers probably reflects that (i) these originate from the same defect and correspond to different charge states (thermal stability of the UK1 and UK2 centers is similar[20]), or (ii) the origin of these is different but simply shows a similar distribution (simulation results show similar distributions for V_C, C_I, V_{S_i}, and Si_I just after the implantation, as mentioned above). In contrast, group B (HK0 and HK2) is distributed to a much deeper region after Ar annealing at 1300 °C than the depth profile of implanted atoms, indicating that the origin of these contains a mobile defect such as C_I and Si_I. The concentration of the HK0 center is about three times higher than that of the HK2 center in the whole monitored area. In other words, the concentration of the HK0 center is different from that of the HK2 center, but the diffusion coefficient of HK0 is the same as that of the HK2, indicating that these could contain the same defect but form different configurations, like C_I, $(C_I)_2$, $(C_2)_{Si}$, $(C_3)_{Si}$, and $((C_2)_{Si})_2$.

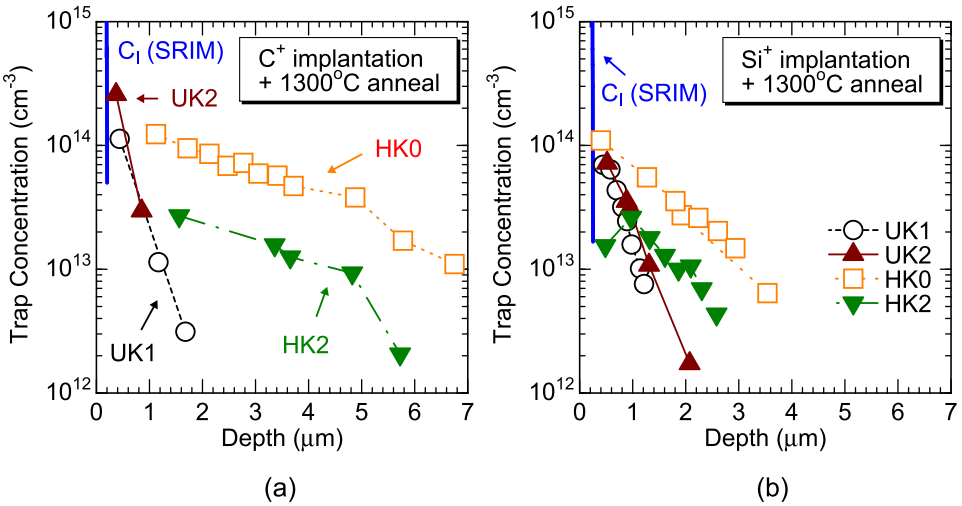

FIG. 12. Depth profiles of deep levels in the p-type 4 H-SiC after (a) C^+ or (b) Si^+ implantation (dose: 1×10^{13} cm^{-2}) followed by Ar annealing at 1300 °C for 20 min. A depth profile of carbon interstitials just after C^+ implantation simulated by SRIM code is also shown as a solid line.

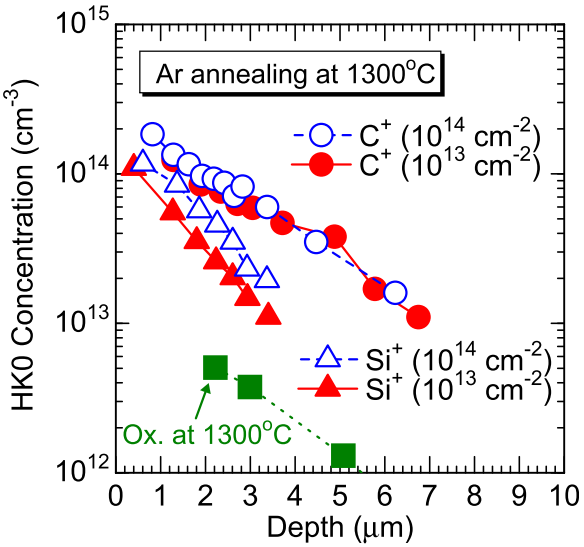

FIG. 13. Depth profiles of HK0 center in the p-type 4H-SiC after C^+ (circles) and Si^+ (triangles) implantation followed by Ar annealing at 1300 °C for 20 min. Depth profile of HK0 center in the sample oxidized at 1300 °C for 20 min is also shown as square symbols.

Figure 13 shows plots of the depth profiles for the HK0 center in the samples after implantation with either C^+ (circles) or Si^+ (triangles) followed by Ar annealing at 1300 °C for 20 min. The HK0 concentration after implantation is clearly higher than that after thermal oxidation at 1300 °C for 20 min (closed squares, dotted line). This should come as a result of the high amounts of interstitials near the surface region induced by ion implantation, either C^+ or Si^+. The HK0 center in C^+-implanted samples is distributed to a deeper region with higher concentration compared with that in Si^+-implanted samples, indicating that the origin of the HK0 center is C_I-related defects. If the HK0 center originates from other defects (e.g., Si_I) generated by implantation bombardment (some of the defects might not recombine and thus diffuse during Ar annealing), the HK0 concentration in the Si^+-implanted samples must be higher than that in the C^+-implanted samples because the amount of displaced atoms in the Si^+-implanted samples is higher than that in the C^+-implanted samples under this implantation condition, as calculated by the SRIM code (Fig. 11). Therefore, the HK0 in the C^+-implanted samples can be determined mainly by the diffusion of implanted carbon atoms (excess carbon atoms), whereas the distribution in the Si^+-implanted samples mainly by diffusion of C_I generated by implantation bombardment. We also investigated the dependence of the HK0 distribution on implantation dose. In Fig. 13, closed/open symbols indicate the HK0 distribution for doses $1 \times 10^{13}\,cm^{-2}/1 \times 10^{14}\,cm^{-2}$. The HK0 concentration in the samples implanted at the higher dose is almost the same or slightly higher than that at the lower dose, suggesting that the amount of C_I diffusion is not much different in the two samples ($1 \times 10^{13}\,cm^{-2}/1 \times 10^{14}\,cm^{-2}$ dose). Because too high a concentration of C_I defects (e.g., $1 \times 10^{18}\,cm^{-3}$) is thermodynamically unfavorable, this concentration should be reduced to a certain level during Ar annealing by either conversion to other defects or diffusion to the sample surface.

IV. DISCUSSION

In this study, eight deep levels, GP1 ($E_V + 0.46$ eV), D ($E_V + 0.63$ eV),[17–20] HS2 ($E_V + 0.63$ eV),[9,20] HK4 ($E_V + 1.4$ eV),[20] UK1 ($E_V + 0.49$ eV),[20] UK2 ($E_V + 0.71$ eV),[20] HK0 ($E_V + 0.79$ eV),[20] and HK2 ($E_V + 0.98$ eV)[20] centers, were detected in p-type 4 H-SiC; a summary is given in Table II. The GP1 center was occasionally detected in as-grown samples (Fig. 1) and disappeared after oxidation at 1400 °C (Fig. 6) or Ar annealing at 1440 °C (not shown). This type of deep level was not found in previous reports. The D center, which has been attributed to B_{Si}-V_C,[18,21,22] was detected in all as-grown samples and disappeared after thermal oxidation (Fig. 1). V_C in the D center will be filled with diffusing C_I emitted from the oxidizing interface. The HS2 and HK4 centers were generated by electron irradiation and disappeared after thermal oxidation at 1150 °C (Fig. 7).

TABLE II. Deep levels observed in p-type 4H-SiC and the condition for generation and elimination. The suspected origins are also shown.

Label	$E_T - E_V$ (eV)	Generated by	Eliminated by	Origin (speculation)
GP1	0.46	As-grown	1440 °C Ar annealing	Unknown
D	0.63		1150 °C oxidation	B_{Si}-V_C[18,21,22]
HS2	0.63	Electron irradiation	1150 °C oxidation or 1350 °C Ar annealing[20]	C-related
HK4	1.4		1150 °C oxidation or 1550 °C Ar annealing[20]	
UK1	0.49	Electron irradiation or C^+/Si^+ implantation	1440 °C Ar annealing	C-related and immobile
UK2	0.71			
HK0	0.79	Oxidation or electron irradiation or C^+/Si^+ implantation	1400 °C Ar annealing	$(C_I)_2$ or $(C_3)_{Si}$ or $((C_2)_{Si})_2$
HK2	0.98			

The HS2 and HK4 centers should be related to C_I or/and V_C, because depth profiles for these after irradiation with 150 keV electrons, causing displacement of only carbon atoms, seem to reflect the irradiation damage (Fig. 8). The UK1 and UK2 centers were generated by electron irradiation (Fig. 7) or C^+/Si^+ implantation (Fig. 10), which remained after Ar annealing at 1300 °C (Fig. 12) but eliminated at 1440 °C (not shown). The depth profiles of the UK1 and UK2 centers followed irradiation damage (Fig. 8) or C^+/Si^+ implantation damage (Fig. 12), and did not change after Ar annealing at 1300 °C (Fig. 12), indicating that these originate from carbon-related and immobile defects.

The HK0 and HK2 centers must be related to interstitials (not vacancy) because (i) the HK0 distribution after oxidation can be fitted by the interstitial distribution calculated from the diffusion equations (1)–(5) (Figs. 2 and 3), and (ii) these centers are distributed to much deeper regions compared with the other deep levels (UK1 and UK2) after C^+ or Si^+ implantation followed by Ar annealing (Fig. 12). In addition, the HK0 and HK2 centers must be carbon-related defects (not silicon-related defect) because (i) these are generated by irradiation with 150 keV electrons, and (ii) higher concentrations of the HK0 and HK2 centers are observed in C^+-implanted samples than in Si^+-implanted samples (Fig. 13); nevertheless, the amount of displaced atoms by Si^+ implantation is higher than that by C^+ implantation. Furthermore, the HK0 and HK2 centers are inferred to be complex defects (not single C_I) from the results that (i) the HK0 center is generated (through diffusion of carbon interstitials) during thermal oxidation, but does not diffuse by subsequent Ar annealing at the same temperature (Fig. 4), and (ii) the HK0 and HK2 centers are not detected just after irradiation, but detected after the subsequent annealing (Fig. 7). From these results, the origin of the HK0 center should be a complex that includes carbon interstitial(s) like $(C_I)_2$, $(C_3)_{Si}$, or $((C_2)_{Si})_2$. This defect should decompose or be converted to other defects at temperatures over 1400 °C (Figs. 6 and 10). PL signals corresponding to these C_I-related complexes have been reported in electron-irradiated SiC,[25,31–37] thermal stability of which is similar to that of the HK0 center.

We speculate that point defects during thermal oxidation should behave as follows. Carbon interstitials (and also silicon interstitials) are generated at the SiO_2/SiC interface and diffuse into SiC bulk during thermal oxidation. The concentration of silicon interstitials in SiC bulk after oxidation is much lower than that of carbon interstitials because of the low diffusivity.[40,41] Many diffusing carbon interstitials recombine with carbon vacancies, leading to a reduction in $Z_{1/2}$ centers. Other carbon interstitials combine with one another (or combine and occupy silicon vacancies) and form C_I-related complexes (the origin of HK0 center) during oxidation when the oxidation temperature is below 1300 °C. Subsequent Ar annealing at over 1400 °C decomposes the source of the HK0 center (and/or form more thermally stable defects). For oxidation at over 1400 °C, C_I defects do not combine with others (or form very thermally stable defects) during oxidation, resulting in no DLTS peaks in the lower half of the bandgap in 4 H-SiC.

V. CONCLUSION

We sought to reveal the origins of the deep levels observed in p-type 4H-SiC after thermal oxidation, especially HK0 ($E_V + 0.79$ eV) and HK2 ($E_V + 0.98$ eV) centers, by comparing deep levels observed in oxidized, electron-irradiated, and C^+- or Si^+-implanted samples. The HK0 and HK2 centers are generated by thermal oxidation, electron irradiation, or C^+/Si^+ implantation, and eliminated by Ar annealing at temperatures over 1400 °C. From this behavior of the HK0 and HK2 centers, the origin of these centers is thought to be from a complex that include carbon interstitial(s) like $(C_I)_2$, $(C_3)_{Si}$, or $((C_2)_{Si})_2$. PL signals corresponding to these C_I-related complexes have been reported in electron-irradiated SiC, the thermal stability of which is similar to that of the HK0 center. Following all results in this study, we could describe the behavior of the point defects (and deep levels) in SiC during oxidation and during subsequent Ar annealing.

ACKNOWLEDGMENTS

This work was supported by the Funding Program for World-Leading Innovative R&D on Science and Technology (FIRST Program) and a Grant-in-Aid for Scientific Research (21226008 and 80225078) from the Japan Society for the Promotion of Science.

[1]D. V. Lang and C. H. Henry, Phys. Rev. Lett. **35**, 1525 (1975).
[2]T. Dalibor, G. Pensl, H. Matsunami, T. Kimoto, W. J. Choyke, A. Schöner, and N. Nordell, Phys. Status Solidi A **162**, 199 (1997).
[3]P. B. Klein, B. V. Shanabrook, S. W. Huh, A. Y. Polyakov, M. Skowronski, J. J. Sumakeris, and M. J. O'Loughlin, Appl. Phys. Lett. **88**, 052110 (2006).
[4]K. Danno, D. Nakamura, and T. Kimoto, Appl. Phys. Lett. **90**, 202109 (2007).
[5]L. Storasta and H. Tsuchida, Appl. Phys. Lett. **90**, 062116 (2007).
[6]L. Storasta, H. Tsuchida, T. Miyazawa, and T. Ohshima, J. Appl. Phys. **103**, 013705 (2008).
[7]T. Hiyoshi and T. Kimoto, Appl. Phys. Express **2**, 041101 (2009).
[8]K. Kawahara, J. Suda, and T. Kimoto, J. Appl. Phys. **111**, 053710 (2012).
[9]L. Storasta, J. P. Bergman, E. Janzén, A. Henry, and J. Lu, J. Appl. Phys. **96**, 4909 (2004).
[10]T. Hornos, A. Gali, and B. G. Svensson, Mater. Sci. Forum **679–680**, 261 (2011).
[11]T. Kimoto, S. Nakazawa, K. Hashimoto, and H. Matsunami, Appl. Phys. Lett. **79**, 2761 (2001).
[12]K. Danno and T. Kimoto, J. Appl. Phys. **100**, 113728 (2006).
[13]N. T. Son, X. T. Trinh, L. S. Løvlie, B. G. Svensson, K. Kawahara, J. Suda, T. Kimoto, T. Umeda, J. Isoya, T. Makino, T. Ohshima, and E. Janzén, Phys. Rev. Lett. **109**, 187603 (2012).
[14]K. Kawahara, X. Trinh, N. Son, E. Janzén, J. Suda, and T. Kimoto, "Investigation on origin of $Z_{1/2}$ center in SiC by DLTS and EPR, 'Tu5-3'," in The 9th European Conference on Silicon Carbide and Related Materials, Saint-Petersburg, Russia, 2012.
[15]T. Miyazawa, M. Ito, and H. Tsuchida, Appl. Phys. Lett. **97**, 202106 (2010).
[16]S. Ichikawa, K. Kawahara, J. Suda, and T. Kimoto, Appl. Phys. Express **5**, 101301 (2012).
[17]T. Troffer, M. Schadt, T. Frank, H. Itoh, G. Pensl, J. Heindl, H. P. Strunk, and M. Maier, Phys. Status Solidi A **162**, 277 (1997).
[18]S. G. Sridhara, L. L. Clemen, R. P. Devaty, W. J. Choyke, D. J. Larkin, H. S. Kong, T. Troffer, and G. Pensl, J. Appl. Phys. **83**, 7909 (1998).
[19]M. Ikeda, H. Matsunami, and T. Tanaka, Phys. Rev. B **22**, 2842 (1980).
[20]K. Danno and T. Kimoto, J. Appl. Phys. **101**, 103704 (2007).
[21]A. Duijn-Arnold, T. Ikoma, O. G. Poluektov, P. G. Baranov, E. N. Mokhov, and J. Schmidt, Phys. Rev. B **57**, 1607 (1998).
[22]P. Baranov, I. Il'in, and E. Mokhov, Phys. Solid State **40**, 31 (1998).

[23]K. Kawahara, M. Krieger, J. Suda, and T. Kimoto, J. Appl. Phys. **108**, 023706 (2010).
[24]M. Bockstedte, A. Mattausch, and O. Pankratov, Phys. Rev. B **69**, 235202 (2004).
[25]A. Mattausch, M. Bockstedte, and O. Pankratov, Phys. Rev. B **70**, 235211 (2004).
[26]A. Gali, N. T. Son, and E. Janzén, Phys. Rev. B **73**, 033204 (2006).
[27]X. Shen, M. P. Oxley, Y. Puzyrev, B. R. Tuttle, G. Duscher, and S. T. Pantelides, J. Appl. Phys. **108**, 123705 (2010).
[28]F. Devynck, A. Alkauskas, P. Broqvist, and A. Pasquarello, AIP Conf. Proc. **1199**, 108 (2009).
[29]T. Hiyoshi and T. Kimoto, Appl. Phys. Express **2**, 091101 (2009).
[30]K. Kawahara, J. Suda, G. Pensl, and T. Kimoto, J. Appl. Phys. **108**, 033706 (2010).
[31]G. A. Evans, J. W. Steeds, L. Ley, M. Hundhausen, N. Schulze, and G. Pensl, Phys. Rev. B **66**, 352041 (2002).
[32]A. Mattausch, M. Bockstedte, O. Pankratov, J. W. Steeds, S. Furkert, J. M. Hayes, W. Sullivan, and N. G. Wright, Phys. Rev. B **73**, 161201 (2006).
[33]J. W. Steeds and W. Sullivan, Phys. Rev. B **77**, 195204 (2008).
[34]J. W. Steeds, W. Sullivan, S. A. Furkert, G. A. Evans, and P. J. Wellmann, Phys. Rev. B **77**, 195203 (2008).
[35]F. Yan, R. P. Devaty, W. J. Choyke, A. Gali, T. Kimoto, T. Ohshima, and G. Pensl, Appl. Phys. Lett. **100**, 132107 (2012).
[36]I. G. Ivanov, A. Gällström, R. Coble, R. Devaty, W. Choyke, and E. Janzén, Mater. Sci. Forum **717–720**, 259 (2012).
[37]A. Gali, P. Deák, P. Ordejón, N. T. Son, E. Janzén, and W. J. Choyke, Phys. Rev. B **68**, 125201 (2003).
[38]J. F. Ziegler, M. D. Ziegler, and J. P. Biersack, Nucl. Instrum. Methods Phys. Res. B **268**, 1818 (2010).
[39]R. Devanathan and W. Weber, J. Nucl. Mater. **278**, 258 (2000).
[40]J. D. Hong and R. F. Davis, J. Am. Ceram. Soc. **63**, 546 (1980).
[41]J. D. Hong, R. F. Davis, and D. E. Newbury, J. Mater. Sci. **16**, 2485 (1981).